Materials and Structures (2024) 57:236
https://doi.org/10.1617/s11527-024-02508-6

ORIGINAL ARTICLE

# Optimised biopolymer-based capsules for enhancing the mechanical and self-healing properties of asphalt mixtures

**Jose Norambuena-Contreras · Jose L. Concha · Gonzalo Valdes-Vidal · Clare Wood**

Received: 23 July 2024 / Accepted: 30 October 2024


**Abstract** The growing need to enhance our road infrastructure has driven the development of several innovative techniques in recent years. Among these advancements, encapsulated rejuvenator solutions for extrinsic self-healing asphalt have emerged as a significant topic of interest. This paper evaluates the effect of optimised capsules containing vegetal oil as a biorejuvenator on the physical, mechanical, and self-healing properties of dense asphalt mixtures. In this study, previously optimised polynuclear alginate-based capsules were synthesised using vibrating jet technology with 5% wt. calcium chloride and a biopolymer-to oil mass ratio 1:7. Optimised capsules were incorporated into the asphalt mixture at concentrations of 0.125% wt., 0.25% wt., and 0.5% wt. Their spatial distribution within the asphalt mixtures was evaluated using an alternative method to CT scans, which utilised machine learning-based image analysis of the core asphalt samples. The main findings of this research are as follows: (1) a uniform distribution of capsules was achieved throughout the asphalt mixture, although clustering was observed at higher concentrations. (2) The capsules successfully survived the asphalt manufacturing process, and mechanical tests highlighted the adhesive properties of the alginate encapsulation material. (3) Asphalt samples with 0.125% wt. capsules exhibited mechanical performance comparable to samples without capsules; however, this content did not significantly enhance their self-healing properties. In contrast, self-healing capabilities were significantly enhanced with a capsule content greater than or equal to 0.25% wt.; however, this enhancement slightly affected some physical–mechanical properties of the dense asphalt mixture.

**Keywords** Vegetal oil · Alginate Capsules · Mechanical properties · Asphalt self-healing

**Supplementary Information** The online version contains supplementary material available at https://doi.org/10.1617/s11527-024-02508-6.

J. Norambuena-Contreras (✉) · C. Wood
Materials and Manufacturing Research Institute, Department of Civil Engineering, Faculty of Science and Engineering, Swansea University, Bay Campus, Swansea SA1 8EN, UK
e-mail: j.norambuena@swansea.ac.uk

C. Wood
e-mail: c.wood@swansea.ac.uk

J. L. Concha
LabMAT, Department of Civil and Environmental Engineering, University of Bío-Bío, 4051381 Concepción, Chile
e-mail: jlconcha@ubiobio.cl

G. Valdes-Vidal
Department of Civil Engineering, Faculty of Engineering and Science, Universidad de La Frontera, Temuco, Chile
e-mail: gonzalo.valdes@ufrontera.cl

Published online: 19 November 2024

## 1 Introduction

Asphalt mixture is the predominant material used for road pavement construction worldwide. Approximately 95% of the total weight of the asphalt mixture is associated with the aggregate, which provides the structural support, whilst the remaining 5% wt. is the bitumen, which is the binding material [1, 2]. Despite the low bitumen proportion in the asphalt mixtures, the continuous exposure of bitumen to variable temperatures and oxygen induces thermo-oxidative ageing, leading to the formation of microcracks [3–5]. From the chemical viewpoint, the thermo-oxidative ageing is explained by the volatilisation of the lighter components of the maltenic fraction in the asphalt bitumen (i.e. saturates and aromatics) which are responsible for dispersing the asphaltenes and providing the bitumen with fluidity. Hence, a reduction of the maltenes will promote the aggregation of the heavier compounds in the bitumen (i.e. resins and asphaltenes) forming clusters [6, 7]. Consequently, the viscosity of the bitumen decreases, causing it to become stiffer and more brittle. This increase in brittleness makes the asphalt mixture more susceptible to cracking, thereby reducing the service life of asphalt roads [8–10]. Given this concern, several research initiatives have been pursued to advance the early-stage self-healing of cracked asphalt pavements [11–14]. Among them, the autonomous approach by the action of encapsulated rejuvenating agents incorporated into the asphalt mixtures has gained great interest [15, 16].

Encapsulated asphalt rejuvenators consist of capsules with spherical morphology containing a rejuvenator liquid, usually a low-viscosity oil with a high maltene content [17, 18]. Such systems have the capacity to induce a restoration of the asphaltene/maltene ratio and recover the viscoelastic behaviour of the aged asphalt bitumen [19]. The capsules are incorporated during the preparation of the asphalt mixture, with the capsule design being such that they remain thermally and mechanically stable during the field mixing and compaction process. Thereafter, during the service life of the asphalt pavement structure, the crack propagation and traffic loads promote the activation of the capsules by rupture or deformation, depending on the capsule type (i.e. polynuclear or core–shell). During activation, the rejuvenator is released, diffusing within the cracked bitumen with a softening effect that decreases its viscosity, so that the bitumen can flow and seal the microcrack autonomously [20, 21].

Over the past decade, extensive research has focused on synthesising capsules with a polynuclear morphology. These capsules are based on a biopolymeric matrix of alginate and contain sunflower oil as a vegetal agent for rejuvenating asphalt. [22–28]. In these polynuclear capsules, sunflower oil is distributed within multiple internal cavities provided by the biopolymeric alginate matrix. This design enables progressive release, facilitating multiple healing events throughout the service life of the asphalt pavement [29, 30]. Because of its excellent thermal and mechanical stability during the mixing and compaction stages of asphalt manufacturing, alginate has been proposed as a viable alternative to formaldehyde-based synthetic polymers, which are often linked to adverse environmental impacts [31]. Meanwhile, virgin cooking oil (VCO), such as sunflower oil, has been suggested as a vegetal-derived rejuvenator that softens and restores the maltenic fraction of aged bitumen, thereby enhancing its rheological properties [32, 33].

Asphalt mixtures must provide a reliable mechanical performance under a broad range of environmental and load conditions. Therefore, any attempts to enhance the self-healing ability of asphalt mixtures using polynuclear alginate-VCO capsules must not compromise the asphalt mixture's mechanical stability. An initial study conducted by Al-Mansoori et al. [34] revealed that adding alginate capsules in amounts ranging from 0.25% wt. to 1.0% wt. of a dense asphalt mixture resulted in comparable water susceptibility, particle loss, and permanent deformation compared to the asphalt mixture without capsules. Later, Norambuena-Contreras et al. [35] found that adding alginate-VCO capsules at a concentration of 0.5% by weight to dense asphalt mixtures did not significantly affect the stiffness modulus of the mixtures. This suggests that the capsules can be added at the end of the mixing process to achieve high levels of self-healing capability. Zhang et al. [36] found that incorporating 0.5% of alginate-VCO capsules per total mass of dense asphalt mixture resulted in the recovery of up to 180% of the fracture energy under fatigue loading. Recently Ruiz-Riancho et al. [37] concluded that the addition of the alginate-VCO capsules in porous asphalt mixtures delays reflective cracking and increases the rutting with the oil released without influencing the skid resistance.

Garcia-Hernández et al. [38] evaluated the self-healing properties of Stone Mastic Asphalt (SMA), porous and dense asphalt mixtures incorporating 0.5% of capsules per total mass of asphalt mixture. This study revealed that self-healing is more effective in porous asphalt mixtures due to the gradual release of encapsulated oil. In contrast, in dense asphalt mixtures, the encapsulated oil is released only when cracks appear. Traseira-Piñeiro et al. [39] proved that alginate-VCO capsules for asphalt self-healing purposes could also resist the mixing process at an industrial-scale asphalt plant, reducing particle loss by up to 25% in porous asphalt mixtures.

Most recently, Concha et al. [40] developed the first study to establish a dosage curve for alginate-VCO capsules aimed at restoring the physical and rheological properties of long-term aged bitumen to a state comparable to short-term ageing. The dosage curve was determined based on the design parameters of the capsules, such as the biopolymer to oil (B:O) mass ratio and the oil payload. For this purpose, the study concluded that an optimal capsule design would be based on a B:O mass ratio of 1:7 incorporated in a content of 0.25% wt. of asphalt mixture. However, the impact of this optimised capsule design and dosage on the mechanical and self-healing performance of asphalt mixtures under various loading and environmental conditions has not been thoroughly investigated. For these reasons, the main objective and novelty of this research is to assess how incorporating an optimised design of alginate-based capsules containing virgin cooking oil as an asphalt bio-rejuvenator affects the physical, mechanical and self-healing properties of dense asphalt mixtures. To do that, standard laboratory procedures were employed to measure the physical and mechanical properties of the asphalt mixtures, whilst a novel experimental mechanical test approach was developed to quantify their self-healing capabilities. Additionally, the spatial distribution of the capsules in varying doses within the asphalt mixture cores was evaluated using machine learning-based image analysis.

## 2 Materials and methods

### 2.1 Materials

Dense asphalt mixtures containing optimised alginate-VCO capsules were prepared in this study. The aggregates used were classified into three fractions; coarse (size: 12.5–5 mm), fine (size: 5–0.08 mm), and filler (size < 0.08 mm); see aggregates gradation in Table 1. According to Chilean specifications [41], a CA-24 type bitumen was used in this study (penetration of 58 dmm, softening point of 51.4 °C). This bitumen can be classified with a PG 64-22. Additionally, an optimised alginate-based polynuclear capsule design was used in this study, see Fig. 1a. The encapsulating matrix of the polynuclear capsules consisted of low-viscosity sodium alginate powder (Mannuronic/Guluronic ratio of 0.77, density 1.02 g/cm$^3$ and viscosity of 175 mPa•s in a 2% wt. solution @20 °C), provided by Gelymar company (Santiago, Chile) and calcium-chloride dihydrate ($CaCl_2 \cdot 2H_2O$) at 77% purity, provided by Winkler (Concepción, Chile). Also, virgin cooking oil (VCO) from a commercially available sunflower oil (density 0.85 g/cm$^3$, viscosity 70 mPa•s @20 °C, pH 5.3–5.5) was selected as the asphalt rejuvenator to be encapsulated.

### 2.2 Synthesis and properties of optimised alginate polynuclear capsules

Based on the previous study carried out by the authors [42], optimised alginate-based capsules were synthesised based on the ionic gelation principle of alginate and $Ca^{2+}$ ions from the $CaCl_2 \bullet 2H_2O$. The method consisted of the following two steps:

(1) *Emulsion preparation:* a 2% wt. sodium alginate solution was prepared by using a magnetic stirrer (Scilogex, Model SCI550-S, Rocky Hill, CO, USA) at 250 rpm for 24 h. Then, the alginate solution was mechanically agitated (Scilogex,

**Table 1** Particle size distribution of the dense asphalt mixture

| Sieve size | Particle size (mm) | % passing |
|---|---|---|
| 3/4" | 20 | 100 |
| 1/2" | 12.5 | 89 |
| 3/8" | 10 | 80 |
| N°4 | 5 | 66 |
| N°8 | 2.5 | 44 |
| N°30 | 0.63 | 22 |
| N°50 | 0.315 | 16 |
| N°100 | 0.16 | 12 |
| N°200 | 0.08 | 9 |

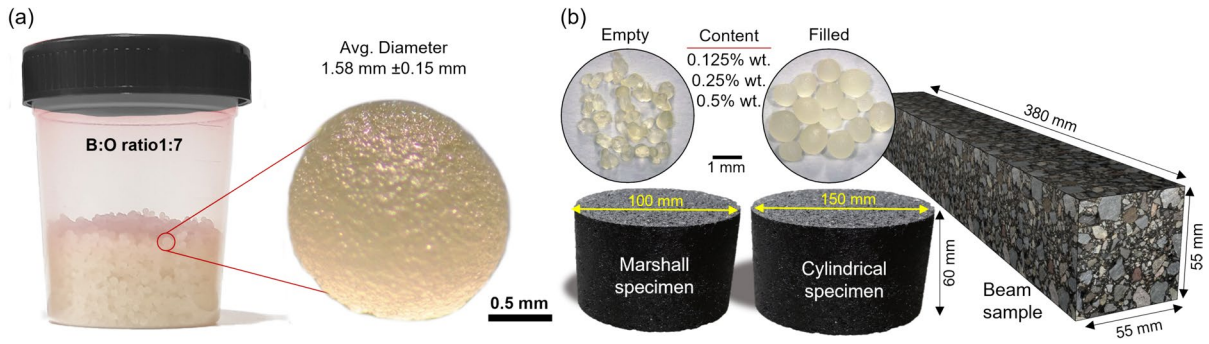


**Fig. 1** **a** Representative image of a synthesised optimised alginate-VCO capsules, and **b** Test samples with empty and filled alginate-VCO capsules. Semi-circular test samples were extracted from Marshall specimens to evaluate the self-healing properties

Model OS40-Pro-LB Pro, Rocky Hill, CO, USA) at 1200 rpm for 40 min, incorporating during this period the VCO at a biopolymer:oil mass (B:O) ratio of 1:7.

(2) *Encapsulation process:* The capsules were produced by the vibrating jet technique recently proposed by the authors to obtain more spherical capsules [43]. For this, an encapsulator Buchi B-390 (Flawil, Switzerland) was used and configured with 450–550 mbar of air pressure and a nozzle of 750 µm coupled to a vibrating unit settled to 350 Hz. The resulting laminar flow emulsion from the nozzle was broken up by vibration, separated into droplets, and collected in a 5% wt. $CaCl_2$ solution agitated at 250 rpm using a magnetic stirrer. To prevent the droplets from hitting each other, an electrostatic charge of 1500 V was applied on the surface of the emulsion droplets. The freshly prepared capsules were filtered from the hardening solution and rinsed with 250 mL of deionised water, then dried in an oven at 30 °C for 24 h. The capsules were stored in a freezer at -5 ºC, preventing the VCO from oxidation. See optimised alginate capsules in Fig. 1a.

Finally, to evaluate the pure effect of the alginate on the mechanical properties of the asphalt mixtures, empty capsules (i.e., B:O ratio 1:0, without VCO) were synthesised following the previous procedure. Table 2 shows the physical, thermal, and mechanical properties of each capsule design.

### 2.3 Manufacturing of dense asphalt mixture adding optimised capsule design

In this study, dense asphalt mixtures with and without optimised alginate-VCO capsules were manufactured in three different geometries: (i) Marshall specimens to measure the properties of stiffness modulus, resistance to cracking at low temperatures, and susceptibility to water damage; (ii) Cylindrical specimens with 150 mm diameter to evaluate the susceptibility to

**Table 2** Properties of the capsules with and without VCO used in this study

| Property | Unit | Empty capsules B:O ratio 1:0 Mean ± Std.Dev | Capsules with VCO B:O ratio 1:7 Mean ± Std.Dev |
|---|---|---|---|
| Size | mm | 0.95 ± 0.017 | 1.572 ± 0.147 |
| Sphericity factor | – | 0.052 ± 0.002 | 0.047 ± 0.004 |
| Encapsulation efficiency | % | – | 94.89 ± 1.187 |
| Encapsulated VCO/g capsule | g | – | 0.558 ± 0.021 |
| Mass loss @160 ºC via TGA | % | 3.9 | 3.5 |
| Compressive strength @20 ºC | MPa | 8.72 ± 0.27 | 4.46 ± 1.06 |
| Compressive strength @160 ºC | MPa | 3.21 ± 0.14 | 0.09 |

permanent deformations via wheel tracking test, and (iii) Slab samples to evaluate the fatigue resistance. In addition, semi-circular test samples were extracted from Marshall specimens to evaluate their self-healing properties. See test samples in Fig. 1b.The manufacturing of each mixture consisted of 4 steps, as follows:

(1) Heating: The aggregates and the respective moulds were heated at 154 °C ± 5 °C for 24 h, while the bitumen was heated at 154 °C ± 5 °C for 2 h before the mixing process.
(2) Mixing: The asphalt mixture was prepared in two batches in metallic bowls compatible with a mixing machine. In the first batch, to be used for the preparation of the Marshall and semicircular samples, the aggregates and bitumen were mixed for a total duration of 1.5 min. In the second batch, to be used for the preparation of slab samples, the aggregates and bitumen were mixed for a total of 45 s, until the aggregates were covered entirely by the binder material. For the addition of the optimised VCO capsules in the Marshall and cylindrical test asphalt samples, VCO capsules were added in contents of 0.0%wt., 0.125%wt., 0.25%wt. and 0.5% wt. of total mass of dense asphalt mixture during the last 15 s of the mixing process. For the slab asphalt samples, a VCO capsule content of 0.125% wt. was added during the 45 s mixing procedure.
(3) Compaction: The asphalt mixtures were poured into the respective preheated moulds. For the Marshall samples, 25 blows on each side of the specimen were applied to test their susceptibility to water damage, whilst 75 blows on each side of the specimen were applied to test their stiffness modulus and resistance to cracking at low temperatures, according to BS-EN 12697–30 [44]. This resulted in test specimens with dimensions of 100 mm diameter and 60 mm height. The cylindrical samples were compacted using a gyratory compactor to reach a void content of 7 ± 1%, resulting in test asphalt samples with dimensions of 150 mm diameter and 60 mm height. The slabs samples manufactured were compacted using a standard asphalt slab roller compactor controlling the compaction energy according to BS-EN 12697–33 [45], resulting in asphalt slabs with dimensions of 50 × 300x400 mm.
(4) Conditioning: Marshall and cylindrical test specimens were conditioned at ambient temperature to be later removed from the mould. A selection of Marshall samples, designed to assess their resistance to cracking at low temperatures, were sectioned into four semi-circular specimens, each measuring 100 mm in diameter, 50 mm in height, and 40 mm in width. These specimens were used to assess the self-healing properties of the asphalt mixtures, both with and without capsules. The asphalt slabs were removed from the mould 20 min after completion of the compaction process. The slabs were then sawn into beam test samples with dimensions 50 × 50x380 mm, according to BS-EN 12697–24 [46].

A total of 65 Marshall specimens, 20 cylindrical specimens and 36 beams were manufactured, see Figure 1b. The asphalt test samples with capsules added at 0.0%, 0.125%, 0.25%, 0.5%, and 1.0% by total weight of the asphalt mixture were labelled as AM-0.0, AM-0.125, AM-0.25, and AM-0.5, respectively. The asphalt mixture with empty capsules was identified as AM-0.25e. Finally, the physical properties of bulk density and the air void content of each type of asphalt mixture were determined under the standards ASTM D-2726-00 [47] and ASTM D-3203-05 [48].

### 2.4 Spatial capsule distribution in asphalt mixtures

The spatial distribution of capsules within the AM-0.125, AM-0.25, and AM-0.5 core test samples extracted from Marshall specimens was analysed using a post-processing image segmentation approach on cross-sections of asphalt mixtures. This machine learning-based image analysis method was proposed as an alternative to computed tomography (CT) analysis. This analysis involved the following four steps:

(1) Test sample preparation: For each Mashall specimen per % capsule content, a cylindrical geometry measuring 55 mm in diameter and 60 mm in height was extracted from the geometric centre of the specimen. Then, to serve as a positional reference, a "V" mark was drawn along the height of each of the extracted cylinders, as shown in Fig. 2a.

(2) Slice cutting: The extracted cylinders were cut into two external discs measuring 15 mm in height and 55 mm in diameter, along with four central discs measuring 5 mm in height and 55 mm in diameter, see Fig. 2b. The central discs were selected for further analysis, considering a 2 mm loss due to sawing. Each of the central discs was labelled with numbers indicating its position and a letter distinguishing the upper face "A" and the bottom face "B". For instance, the upper face of the first disc coming from a sample AM-0.5 was labelled as AM-0.5-1A.
(3) Capsule identification: VCO capsules on each face of the discs were identified and marked for easy spatial location, see Fig. 2c. Then, several high-resolution photographs were taken of both faces of the resulting discs.
(4) Post-processing images: The images were post-processed in ImageJ® software (Fiji distribution, version 1.54b, National Institutes of Health, Bethesda, MD, USA). The Trainable Weka Segmentation tool, driven by machine learning, classified the disc components (i.e., aggregates, voids, and capsules). Therefore, Cartesian coordinates (x, y, z) were employed to denote the spatial position of VCO capsules relative to a shared reference point outside the discs. Here, x and y denote horizontal and vertical coordinates, respectively, while z indicates height, determined by the position and thickness of each disc. The 3D spatial distribution for VCO capsules and distance from the geometrical centre of the cylinder (Dc) were reconstructed using OriginPro 2022 software, v9.95-2022b (OriginLab, Northampton, MA, USA).

## 2.5 Mechanical characterisation of dense asphalt mixtures

The stiffness modulus ($S_M$) of the asphalt mixtures was measured using the indirect tensile strength (ITS; see Fig. 3) test according to the standard BS-EN 12697–26 (annex C) [49]. This involved applying sinusoidal load pulses and rest periods to induce controlled horizontal in three Marshall specimens for each design type. The test was conducted at 20ºC applied ten vertical load cycles to two orthogonal diameters using an Asphalt Mix Performance Tester (GCTS, model ATM 100, Tempe, AZ, USA). $S_M$, in MPa, was determined using Eq. (1):

$$S_M(MPa) = \frac{F \times (v + 0.27)}{(z \times h)} \quad (1)$$

where $F$ is the maximum vertical load applied in N; $v$ is the Poisson ratio (0.35); $z$ is the horizontal strain amplitude in mm; and $h$ is the average thickness of

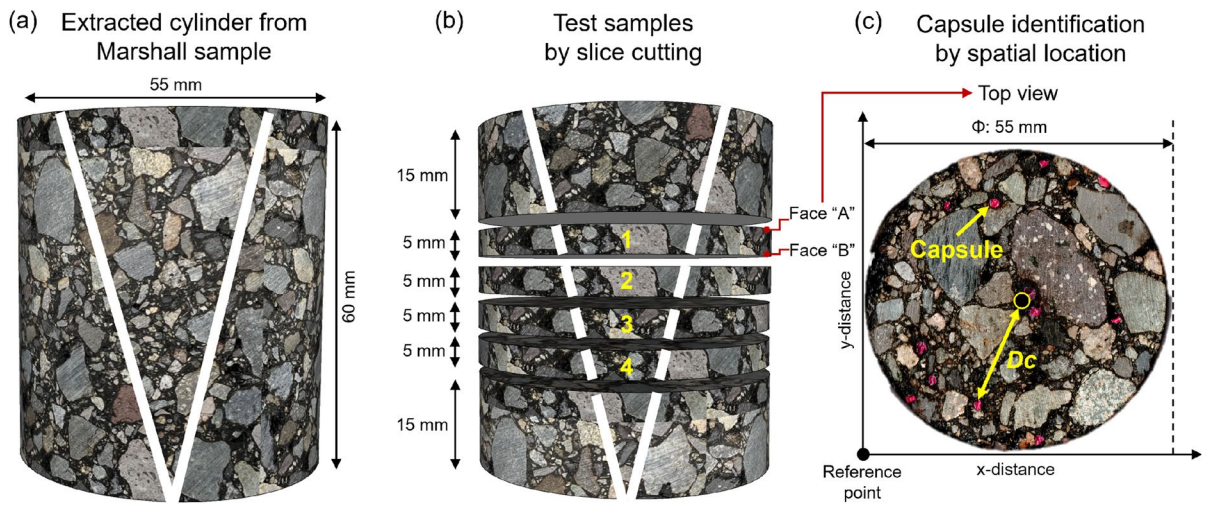


**Fig. 2** Representation of the extracted cylinder from a Marshall sample and its slice-cutting process for analysis of the spatial distribution of VCO capsules. Capsules highlighted in magenta

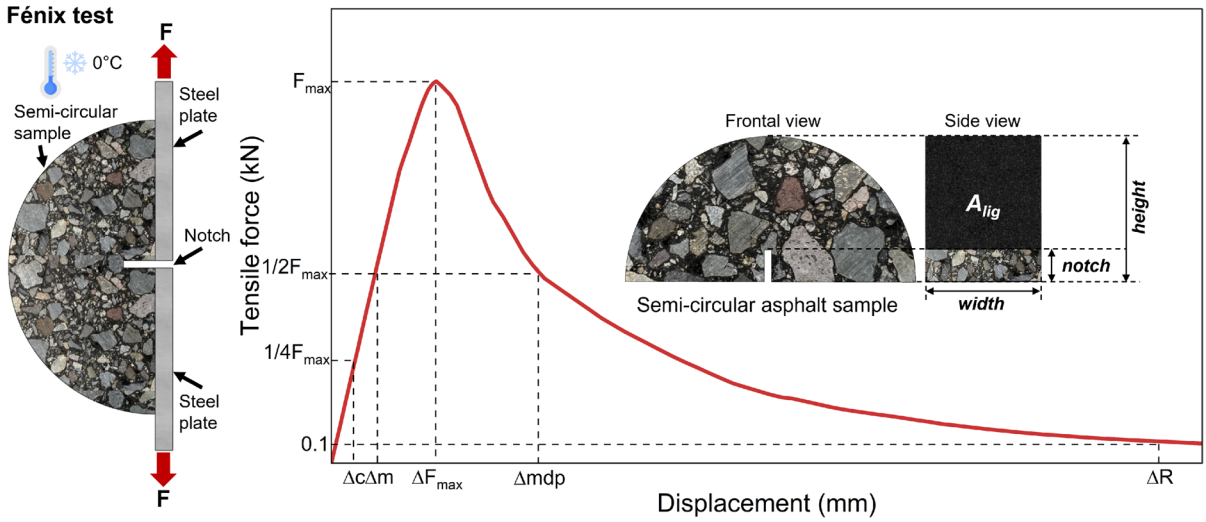


**Fig. 3** Representation of the Fenix test and its resultant load–displacement curve

the specimen in mm. A representative $S_M$ value for each mixture design was determined from the average of 6 measurements.

In addition, the resistance to low-temperature cracking was evaluated using the Fenix test, according to the method applied by Valdes-Vidal et al. [50]. To accomplish this, four semicircular samples of each type of asphalt mixture were conditioned at 0 °C for 4 h. These test samples, fixed between steel plates, underwent testing on an Asphalt Mix Performance Tester (GCTS, model ATM 100, Tempe, AZ, USA), applying a vertical load at a rate of 1 mm/min, see [50]. Force and displacement were recorded until a force value of 0.1 kN after the maximum force ($F_{max}$), determining the following mechanical parameters:

- Maximum tensile force ($F_{max}$): Maximum force resisted by the samples under tensile load, in kN.
- Tensile Stiffness Index ($TSI$): Indicator of the asphalt mixtures' stiffness, determined as:

$$TSI(kN/mm) = \frac{1/2 \times F_{max} - 1/4 \times F_{max}}{(\Delta m - \Delta c)} \quad (2)$$

Where $F_{max}$ is the maximum load, in kN; $\Delta m$ is the displacement before maximum load at 1/2 $F_{max}$, in mm; and $\Delta c$ is the displacement before maximum load at 1/4 $F_{max}$, in mm.

- Dissipated energy per unit area ($G_D$): The mixtures' internal cohesive force, determined as:

$$G_D(J/mm^2) = \frac{\int_0^{\Delta R} F(x)dx}{A_{lig}} \quad (3)$$

where $F$ is the load in, kN; $x$ is the displacement, in mm; $\Delta R$ is the fracture displacement at $F = 0.1$ kN post-peak load, in mm; and $A_{lig}$ is the fracture area, in $m^2$.

- Toughness index ($T_I$): It represents the ability of the mixture components to hold together once the failure has started, calculated as:

$$T_I(J \times mm/m^2) = \frac{\int_{\Delta Fmax}^{\Delta R} F(x)dx}{A_{lig}} \times \left(\Delta_{mdp} - \Delta_{Fmax}\right) \quad (4)$$

where $\Delta_{Fmax}$ is the displacement at $F_{max}$, in mm; and $\Delta_{mdp}$ is the displacement after maximum load at 1/2 $F_{max}$, in mm. Finally, the representative value of each parameter was calculated from the average of 4 measurements (Fig. 3).

The susceptibility to water damage was evaluated by Indirect Tensile Strength ($ITS$) tests according to the standard BS-EN 12697-23 [51], determining the Indirect Tensile Strength Ratio ($ITSR$), according to the BS-EN 12697-12 [52] under dry and wet conditions. For this, three Marshall specimens were used

for each condition and tested in a Marshall testing machine (Matest, model B042-01, Treviolo, Italy). The subgroup for dry *ITS* was kept in air at 20 ± 5 °C, while the subgroup for wet *ITS* was saturated in distilled water and then immersed in a water bath at 40 °C for 68 to 72 h. Then, for both dry and wet conditions, the samples were conditioned at 15 °C, and the *ITS* and *ITSR* were determined according to Eqs. (5) and (6):

$$ITS(GPa) = \frac{2 \times P}{\pi \times D \times H} \quad (5)$$

$$ITSR(\%) = \frac{ITS_w}{ITS_d} \times 100 \quad (6)$$

where $P$ is the maximum applied load, in kN; $D$ is the sample diameter, in mm; $H$ is the sample height, in mm; $ITS_w$ is the indirect tensile strength of the wet sample, in kPa; and $ITS_d$ is the indirect tensile strength of the dry test sample, in kPa. Finally, the representative values of *ITS* and *ITSR* parameters were calculated as the average of 3 measurements per type of mixture.

Rutting performance was evaluated using a Double Wheel Tracker test device (Controls, Model 77-PV33B05, Liscate, Italy) according to AASHTO T 324:2019 [53]. The test involved measuring the depth of the tread formed in paired cylindrical mixture samples immersed in water by repeated loading. First, the test samples were pre-conditioned in a water bath at 50 ± 0.5 °C for 30 min before the test. Then, a concentrated load was applied on the samples consisting of an oscillating movement of a steel wheel loaded with 705 ± 4.5 N at a speed of 26 passes/min. Relevant data were recorded after 10,000 cycles (or 20,000-wheel passes) or when a permanent vertical deformation of 20 mm was reached on the sample test surface. The representative rutting parameters were calculated based on an average rutting curve of 2 measurements per type of asphalt mixture.

Additionally, the fatigue damage of each mixture was evaluated using the 4-point bending test, according to the BS-EN 12697-24 standard (annex D) [46], under deflection control mode. First, each prismatic sample was kept for 24 h in a thermostatic chamber at the test temperature (20 °C). Using a Servo-Pneumatic Four Point Bend Apparatus (IPC Global, model MkIV, Liscate, Italy) the prismatic beams were subjected to periodic stresses under controlled temperature conditions at 20 °C and a frequency of 30 Hz. The applied deflections were 150, 190, and 300 µm/m measured at the centre of the asphalt beam. The fatigue failure criterion adopted was the number of cycles needed for a drop of the initial stiffness modulus by 50% ($N_{f50}$). The fatigue curve was obtained from analytical interpolation of the data registered using the power function shown in Eq. (7):

$$\varepsilon = a \times {N_{f50}}^{-b} \quad (7)$$

where $\varepsilon$ is the value of the initial strain, in µm/m; $a$ and $b$ are interpolation coefficients related to the mixture type; and $N_{f50}$ the number of loading cycles or repetitions of the sample up to the failure criterion. The representative parameters of fatigue including the fatigue laws were calculated as the average of 6 measurements per deflection on each type of asphalt mixture.

### 2.6 Self-healing properties of the asphalt mixtures

Based on the cyclic method proposed by Norambuena-Contreras et al. [35], a modified test recently published by the authors [54] was used to quantify the crack-healing properties in semi-circular asphalt samples by effect of the polynuclear capsules activated by a deformation mode. To achieve this, each semi-circular sample was tested using a three-step fracture-activation-healing process, see Fig. 4. For the first (fracture) step, each semi-circular sample was conditioned to − 5 °C for 2 h to generate a brittle fracture under a 3-point bending test carried out at a load speed of 5 mm/min. The second (activation) step consisted of the activation of the capsules inside the fractured semi-circular samples using a confined compression test applying a compressive load during 60 s counted from a pre-load of 0.5 kN. The third (healing) step required the conditioning of the semi-circular samples at room temperature during 24 h, after which the first step (fracture) was then repeated. With this method, a self-healing index (*HI*) was determined using the Eq. (8):

$$HI(\%) = \left(\frac{F_h}{F_i}\right) \times 100 \quad (8)$$

where $F_i$ is the maximum initial force recorded by the sample before healing in kN, and $F_h$ is the maximum

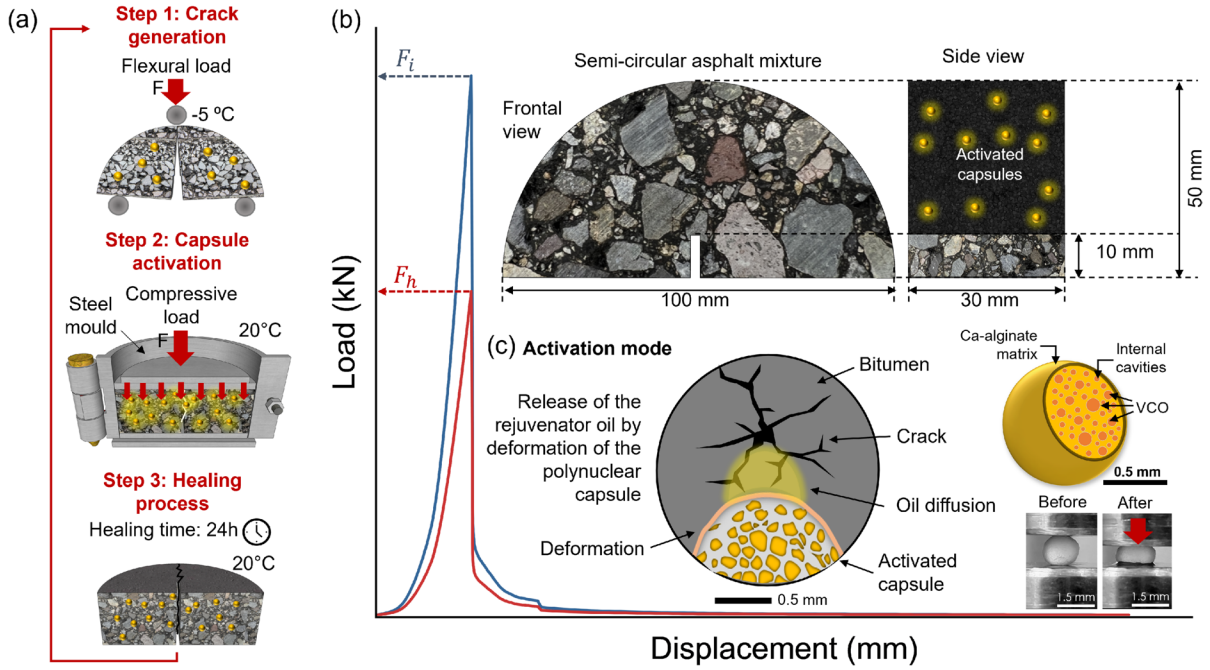


**Fig. 4** Representation of **a** the cyclic crack-healing test process, **b** the compressive load–displacement curve identifying the maximum load before ($F_i$) and after ($F_h$) the healing process, and **c** activation mode of the capsule by deformation

force recorded by the same test sample after the healing process, in kN, see Fig. 4. The representative healing index of each sample was determined as the average of 10 measurements.

### 2.7 Statistical analysis

Statistically significant differences in the physical, mechanical, and self-healing properties of the asphalt mixtures by the effect of the capsule addition were analysed by Analysis of Variance (ANOVA) (Fig. 6). The physical, mechanical (i.e., stiffness, resistance to low-temperature cracking, fatigue), and self-healing properties (i.e., healing indexes) of the asphalt mixtures were evaluated under one-way ANOVA, evaluating the effect of the capsule content (4 levels: 0.0%, 0.125%, 0.25%, and 0.5% wt.). The susceptibility to water damage was evaluated under two-way ANOVA, using a 2×4 general factorial design considering the capsule content in four levels and the type of conditioning (2 levels—dry and wet). Statistical analysis was done with a significance level(α) of 0.05. Pairwise means comparisons were evaluated using the Tukey post-hoc test and represented by grouping capital letters (*A*, *B*, *C*, etc.), where mean values that do not share a letter can be considered as significantly different ($p$-value < 0.05), see Fig. 7b, 8a, and 10. All the statistical analysis was performed by the software OriginPro 2022, version 9.95-2022b (OriginLab, Northampton, MA, USA).

## 3 Results and discussion

### 3.1 Spatial distribution of capsules inside asphalt mixtures

Figure 5 shows the spatial distribution of the VCO capsules inside the asphalt mixtures (a) AM-0.125, (b) AM-0.25, and (c) AM-0.5, observing a total of 41, 93, and 142 capsules, respectively. Since the representative mass of a single capsule is estimated at $2.578 \times 10^{-3}$ g, the capsule mass dosage added in the AM-0.125, AM-0.25, and AM-0.5 Marshall samples was about 1.375 g, 2.75 g, and 5.50 g, respectively. Consequently, the proportion of observed capsules in the asphalt core cylinders for AM-0.125, AM-0.25,

and AM-0.5 was 7.7%, 8.73%, and 6.65%, respectively. These values can be considered comparable to those obtained from previous studies using the CT scan technique [35].

Thus, Fig. 5a shows that the AM-0.125 sample presented a high capsule concentration for the first 10 mm height, identifying two groups (clusters) of capsules. Elsewhere in the sample the capsules were dispersed heterogeneously throughout the cylindrical volume. The AM-0.25 sample in Fig. 5b shows a more homogeneous distribution of capsules in the cylindrical volume. Nonetheless, more groups of capsules are formed compared to the AM-0.125 sample. Figure 5c shows that the AM-0.5 sample presented a capsule distribution concentrated in the middle portion of the cylinder (10–18 mm height), resulting in more groups of capsules than the AM-0.25 sample.

Overall, these groups are composed of a high number of capsules, which increase in number in proportion with the overall capsule concentration in the asphalt mixture. From the previous analysis, it is concluded that the capsules exhibit better dispersion within the volume of the asphalt mixture as their content increases. However, this also leads to the formation of more capsule clusters. Supplementary information shows an animation of the 3D spatial distribution of the capsules inside the samples AM-0.125, AM-0.25, and AM-0.5.

Additionally, Fig. 5 presents the histograms of the distance-to-centre (Dc) of the VCO capsules fitted to a Weibull distribution for the asphalt mixtures (d) AM-0.125, (e) AM-0.25, and (f) AM-0.5. The Weibull distribution can be associated with the stochastic process governing the distribution of capsules within each test sample [55]. Overall, these histograms show a probability of 50% of finding VCO capsules at a Dc up to 16.4 mm, 18.6 mm, and 16.5 mm, respectively. These distances exceed Dc/2 (≈13.8 mm), suggesting that the majority of VCO capsules are situated on the outer half of the cylinder. Refer to the top view of the cylinder alongside each histogram for visual clarification. Based on this analysis, it is evident that the groups of capsules predominantly reside in the outer region of the asphalt mixture. Furthermore, the content and distribution of these capsules play a significant role in influencing the mechanical and self-healing capabilities of asphalt mixtures. Conversely, heterogeneous distribution of capsules could result in potential anisotropic mechanical behaviour, contributing to increased variability in these properties. As has been previously demonstrated [24, 35], the self-healing properties heavily rely on both the content and distribution of the capsules. For example, higher capsule contents can enhance the healing capability of the mixture. Nonetheless, a heterogeneous capsule distribution in the asphalt matrix could lead to capsule activation in a zone where the cracking damage is not occurring, decreasing the overall healing ability in the damaged area. These aspects will be covered in the following sections.

### 3.2 Effect of capsule content on the physical and mechanical properties of asphalt mixtures

Figure 6a shows a dispersion graph with the results of bulk density, air voids, and the stiffness modulus ($S_M$) for each tested sample. Regarding physical properties, this figure illustrates that adding capsules to asphalt mixtures increases their density and reduces their air void content compared to a reference asphalt mixture without capsules. For instance, the average bulk density and air voids of the reference mixture were 2.418 g/cm$^3$ and 3.022%, respectively, while for AM-0.5, they were 2.445 g/cm$^3$ and 1.932%. These variations in bulk density due to the addition of capsules were attributed to changes in the total volume of the samples rather than changes in their total mass.

Additionally, comparing mixtures with capsules showed a decrease in bulk density and consequently an increase in air voids content as the capsule dosage was increased. This phenomenon can be explained by the formation of clusters of capsules at higher dosages, as discussed in the previous section, Fig. 5, which increases the total volume of the mixture. From this initial analysis, it can be concluded that the addition of capsules primarily led to densification of the asphalt mixtures overall.

Regarding the effect of the capsules on the stiffness modulus $S_M$ property, Fig. 6a shows two distinctive effects: i) a stiffening effect for capsule addition up to 0.125% wt. and ii) a softening effect, for capsule addition of 0.25% wt. and 0.5% wt. These effects can be attributed to the influence of each component of the capsules (i.e., the Ca-alginate matrix and the VCO rejuvenator) on the bituminous material, see details of the capsule in Fig. 4c. Similarly, the average $S_M$ results showed in Fig. 6b reveals a tendency for

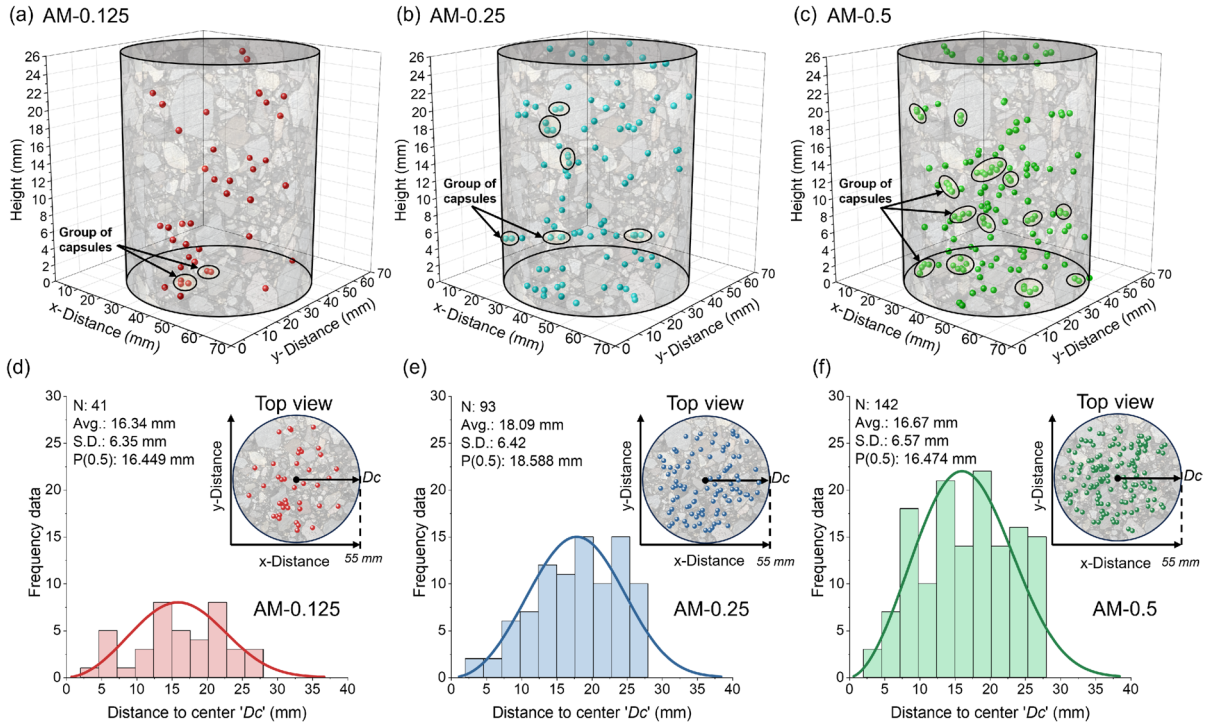


**Fig. 5** **a–c** Spatial capsule distribution and **d–f** Histograms of distance "*Dc*" fitted to Weibull distribution for the asphalt mixtures AM-0.125, AM-0.25, and AM-0.5 (N: number of capsules, Avg: Average value, S.D: Standard deviation, P(0.5): 50% probability)

this property to decrease with the capsule addition, from 4233.6 MPa to 3007.6 MPa for the AM-0.0 and AM-0.5 samples, respectively. Particularly, variations of $S_M$ for the AM-0.125, AM-0.25, and AM-0.5 samples compared to the AM-0.0 were + 8.22%, -18.60%, and -28.95%, respectively. The progressive decrease in $S_M$ for mixtures with capsules is attributed to a partial oil release from the capsules, leading to a greater softening effect in the bitumen. Since $S_M$ was assessed under non-destructive testing conditions, it is hypothesised that partial activation of the capsules occurred during the manufacturing of the asphalt mixtures.

Regarding the effect of the alginate biopolymer on the $S_M$ values, Fig. 6b shows the average $S_M$ for the AM-0.25e test sample with a value of 4393.8 MPa, corresponding to a variation of + 3.78% compared to a reference mixture, indicating a stiffening effect provided by the alginate biopolymer inside the asphalt matrix. Comparing the AM-0.25e and AM-0.25 samples, it is seen a reduction in $S_M$ of − 21.57%, meaning that the encapsulated oil had a softening effect in the rigid matrix of alginate, facilitating the oil release and reducing the $S_M$ of the asphalt mixture. Additionally, the one-way-ANOVA results indicated significant statistical differences ($P$-value < 0.001) for the $S_M$ property. From Fig. 6b, samples not sharing a letter indicate statistically significant differences in $S_M$. From this, an A-group, enclosing the AM-0.0, AM-0.125, and AM-0.25e samples, and B-group enclosing the AM-0.25, and AM-0.5 test samples can be identified. With these results, it is concluded that the $S_M$ value for the AM-0.125 sample was dominated by stiffening effect of the alginate biopolymer, while the $S_M$ values for the AM-0.25 and AM-0.5 samples were dominated by the softening effect of the oil partially released from the capsules during the manufacture of the asphalt mixtures, see Fig. 6b.

Concerning the crack resistance of the asphalt mixtures at low temperatures (0 °C) evaluated by the Fenix test, Fig. 7a shows the average results of maximum force ($F_{max}$), displacement after $0.5F_{max}$ ($\Delta_{mdp}$) and tensile stiffness index ($TSI$). In reference to the effect of adding capsules to an asphalt mixture, it can be observed i) a reduction in $F_{max}$ ranging from − 5% and − 30%, (ii) a reduction of $TSI$ between − 13% and − 19%, and (iii) an increase of $\Delta_{mdp}$ between + 5%

and + 30%. These variations were proportional to the number of capsules added to the asphalt mixture. Consequently, the asphalt mixtures with capsules tended to exhibit decreased resistance to cracking at lower temperatures, displaying more ductile behaviour, and reduced stiffness due to the addition of a softer material. Also, Fig. 7a presents the average results of $F_{max}$, $\Delta_{mdp}$, and *TSI* parameters for the AM-0.25e sample, with variations of + 37.9%, − 19.2%, and + 6.5% compared to the AM-0.25 sample. Such variations indicate a stiffening effect provided by the alginate biopolymer to the asphalt matrix, which is reduced with the incorporation of the VCO (working as a softening agent) partially released during the manufacture of the asphalt mixtures, as previously evidenced by modulus $S_M$ results.

One-way ANOVA results showed statistically significant differences for the $F_{max}$ ($P$-value < 0.001) and $\Delta_{mdp}$ ($P$-value = 0.03) parameters, while not significant differences for *TSI* ($P$-value = 0.67) were identified, see pairwise means comparisons represented by grouping letters in Fig. 7a. Comparing the AM-0.0 sample with those incorporating capsules (AM-0.125, AM-0.25, AM-0.5), statistically significant differences were only identified in $F_{max}$ for asphalt mixtures with capsule contents starting from 0.25% wt., indicating a significant softening effect of the VCO. Also, taking as a reference the AM-0.25e sample, One-way ANOVA revealed statistically similar results with the AM-0.125 and AM-0.25 samples, meaning that the softening effect of the oil partially released from the capsules had no significant effect on $F_{max}$, $\Delta_{mdp}$, and *TSI* parameters. This phenomenon can be explained by the adhesive properties of the alginate biopolymer, a natural water-soluble polysaccharide extracted from some brown algae cell walls. This biomaterial partially mitigates the softening effect of the oil released into the asphalt mixture when the capsule content is increased.

Furthermore, Fig. 7b shows the average results of the dissipated energy ($G_D$) and the toughness index ($T_I$) of the asphalt mixtures under study. Regarding the effect of the capsule addition in the asphalt mixtures, it is observed a reduction of $G_D$ between − 0.5% to − 18%, and an increase of $T_I$ between + 9.0% and + 80.4% compared to the AM-0.0 sample. As a result, asphalt mixtures containing VCO capsules required less energy to crack and displayed more ductile behaviour after reaching their maximum strength. One-way ANOVA results showed statistically

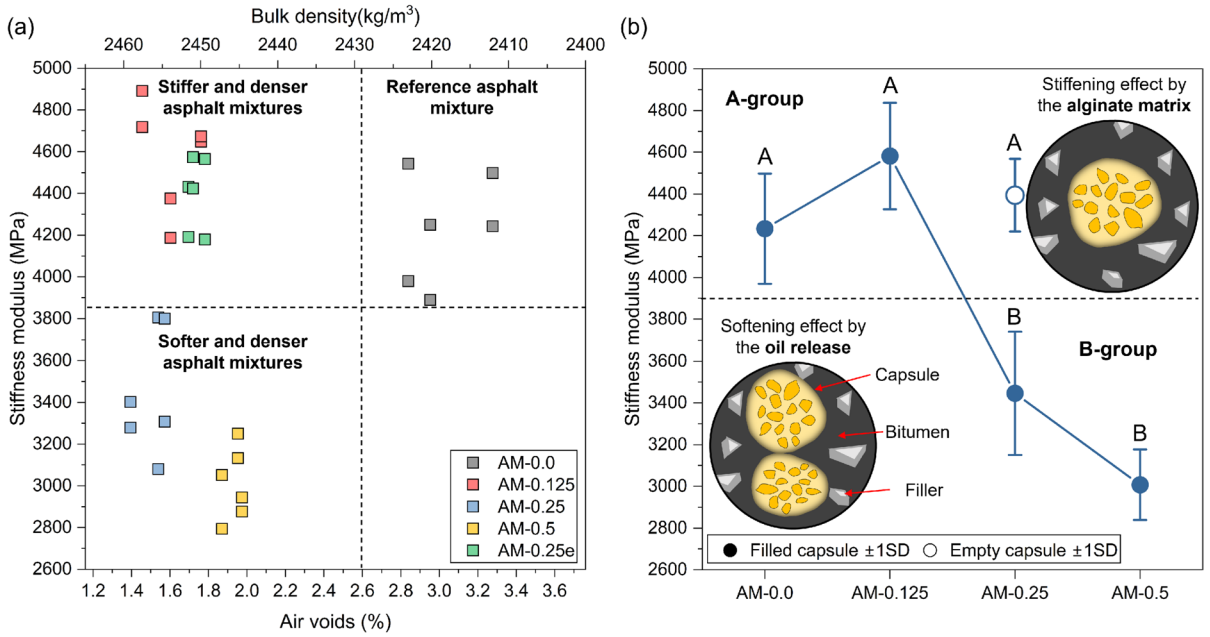


**Fig. 6** **a** Results of bulk density, air voids, and stiffness modulus for each mixture design; and **b** Average results of stiffness modulus for each mixture design. Mean values not sharing a capital letter (*A*, *B*, *C*, etc.) are statistically significant different ($p$-value < 0.05)

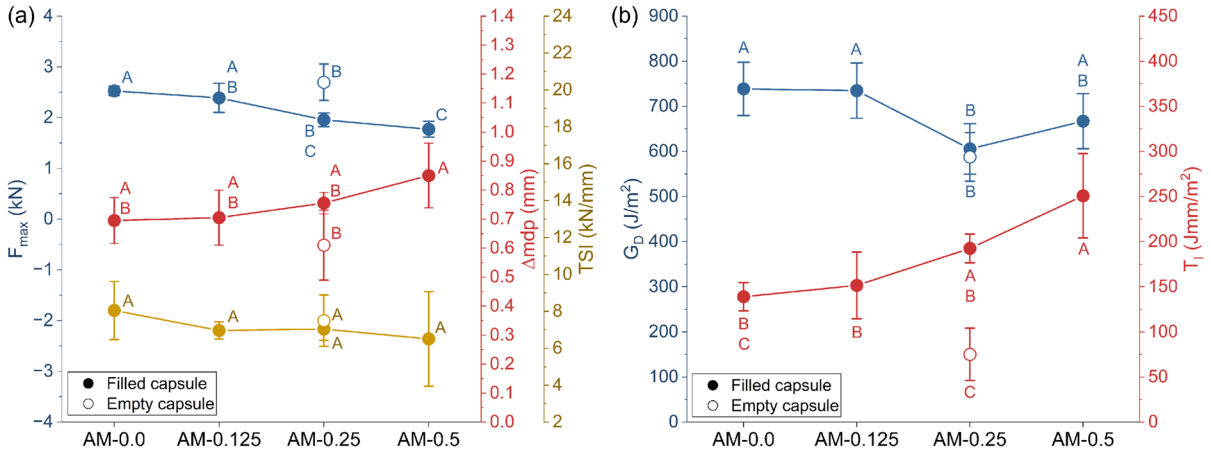


**Fig. 7** Average results of (a) maximum force ($F_{max}$) and tensile stiffness index ($TSI$); and (b) dissipated energy per unit area ($G_D$) and toughness index ($T_I$). Mean values not sharing a capital letter ($A$, $B$, $C$, etc.) are statistically significant different ($p$-value < 0.05)

significant differences for $G_D$ ($P$-value = 0.005) and $T_I$ ($P$-value < 0.001) parameters, see the pairwise mean comparison in Fig. 7b.

Overall, statistically significant differences were appreciated for capsule dosages starting from 0.25% wt. The similar $G_D$ values between the AM-0.25e and AM-0.25 suggest similar energy to achieve cracking, so the softening effect of the oil partially released from the capsules was compensated by the bio-adhesive effect of the alginate matrix. Nonetheless, the significantly lower $T_I$ value for the AM-0.25e compared to the AM-0.25 one suggests that the bio-adhesive effect of the alginate mostly dominated until $F_{max}$. Then, the softening effect of the oil take place, increasing the ductile behaviour of the asphalt mixture. The previous analysis indicates a significant decrease in crack resistance of the mixtures at low temperatures for capsule dosages above 0.125% wt. This is characterised by lower energy required to achieve cracking and more ductile behaviour after mechanical failure due to the softening effect of the VCO partially released from the capsules.

Conversely, the water damage susceptibility of the mixtures (with and without capsules) is proven in Fig. 8a, showing the average values of Indirect Tensile Strength (ITS) under dry (ITSd) and wet (ITSw) conditions. Overall, the ITS of the mixtures decreased with the addition of VCO capsules and after wet conditioning, compared to the ITS values of the respective reference mixtures.

The decrease of ITSd values with the addition of VCO capsules can be attributed to the softening effect of the VCO partially released as increased the capsule dosage. The additional decrease of ITSw with the addition of capsules is explained by the induction of a rubbery and softer behaviour in the encapsulating alginate matrix. This is attributed to the glass transition temperature of the alginate close to the testing temperature of 40 °C [56] summed to the hydrophilic nature of the alginate [57], reducing its adhesive property. This is verified when comparing the AM-0.25 and AM-0.25e test samples (i.e., ITS results in samples with and without VCO), where the higher ITSd and ITSw values for the mixture with empty capsules suggest an adhesive effect of the alginate biopolymer into the asphalt matrix, as previously identified by the Fenix test results (see Fig. 7).

Additionally, Fig. 8b presents the Indirect Tensile Strength Ratio ($ITSR$) values for each mixture design. It is seen a decrease in the $ITSR$ values in the asphalt mixture with the addition of capsules (with and without VCO), evidencing their softer nature compared to the rest of the components of the asphalt matrix. Comparing the $ITSR$ values of the AM-0.0, AM-0.25, and AM-0.25e samples, it is seen a drop of 16% on the $ITSR$ when compared to the AM-0.0 and AM-0.25e samples. Nonetheless, a drop of 9% is registered on the $ITSR$ when compared to the AM-0.0 and AM-0.25 samples. These variations indicate that adding VCO inside the capsules counteracted the

**Table 3** ANOVA *p*-values of the main factors and their interactions on the ITS property

| Variable | ITS *p*-value | Significant differences |
|---|---|---|
| X | < 0.001 | AM-0.25e–AM-0.125(0.25; 0.5)<br>AM-0.0–AM-0.125(0.25; 0.5)<br>AM-0.5–AM-0.125(0.25) |
| Y | < 0.001 | Dry–Wet |
| X*Y | 0.0251 | *see Fig. 8 |

X: capsule content (0.0, 0.125, 0.25, 0.5); Y: conditioning (dry, wet)

softening effect caused by the alginate matrix under wet conditions at a temperature of 40ºC.

Table 3 summarises the ANOVA *p*-values and pairwise means comparison of the ITS values by the effect of the capsule addition and conditioning state. From this Table, it is seen that the capsule content, the conditioning (dry–wet), and their interactions were statistically significant on ITS values. Regarding the effect of the capsule content, Table 3 revealed statistically significant differences except for the AM-0.25e–AM-0.0 and AM-0.25–AM-0.125 pairwise mean comparisons. The statistically similar values for the AM-0.0 and AM-0.25e samples allow to conclude that the alginate biopolymer worked as an adhesive/binder material inside the asphalt matrix rather than a stiffening material under this load condition. As well, the statistically similar ITS values between AM-0.25–AM-0.125 samples evidence no sensibility in changing the ITS values when doubled the initial capsule dosage. So, the softening effect of the VCO partially released from the AM-0.25 sample was balanced by the adhesive effect of the alginate.

To better understand the interaction between factors, Fig. 8a also shows the Tukey-post hoc analysis by grouping letters. Overall, no significant differences are noted when comparing the ITSd and ITSw for the same capsule dosage, except for AM-0.25e samples. The fact that the differences between ITSd and ITSw were significant for the AM-0.25e samples but not for the AM-0.25 sample means that the softening of the alginate under wet conditions was counteracted by the addition of VCO in the alginate matrix. In conclusion, based on the previous analysis, the addition of capsules led to a decrease in the Indirect Tensile Strength (ITS) of the asphalt mixtures under both dry and wet conditions, attributed to the softening effect of the VCO released from the capsules. This reduction was more pronounced under wet conditions, as the additional softening compromised the adhesive properties of the alginate biopolymer when exposed to water.

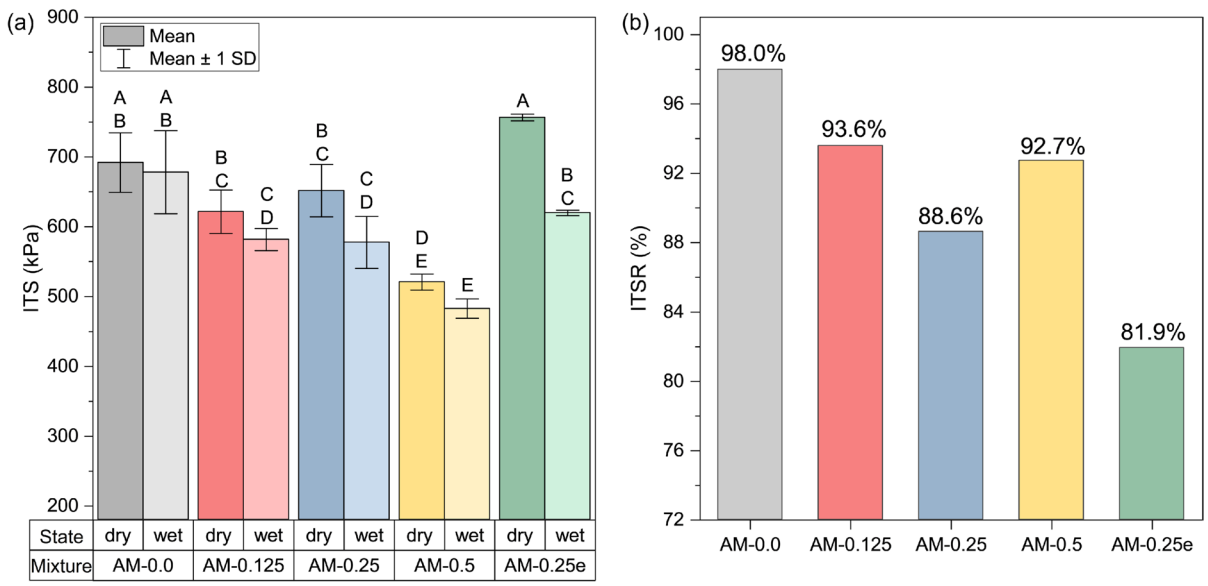


**Fig. 8** Average results of **a** Indirect Tensile Strength (*ITS*) under dry and wet conditions and **b** Indirect Tensile Strength Ratios (*ITSR*) for each of the asphalt mixtures studied. Mean values not sharing a capital letter (*A*, *B*, *C*, etc.) are statistically significant different (*p*-value < 0.05)

Continuing with the effect of capsules on the mechanical behaviour of mixtures containing capsules, Fig. 9 shows the results of wheel tracking tests in the asphalt mixtures with and without VCO capsules. In Fig. 9a the evolution of the Rutting Depth (RD) can be seen in relation to the number of cycles used for the wheel tracking test. The results show that, at 10,000 cycles, the AM-0.125, AM-0.25, and AM-0.5 mixtures presented RD values higher than the reference mixture by + 22%, + 22% and + 28%, respectively. From this, the mixtures with VCO capsules reached RD values up to 50% of their initial height, as seen by the Percentage of Rutting Depth (PRD) in Table 4 determined as the ratio between RD and the initial height of the samples.

Table 4 also shows the results of the Wheel Tracking Slope (WTS) determined between 5000 and 10,000 cycles. It is seen that the WTS parameter decreased from 3.807 mm/$10^{-3}$ to 0.490 mm/$10^{-3}$ as the content of VCO capsules in the asphalt mixtures increased from 0.125% wt. to 0.5% wt., respectively. The decrease in WTS is explained by the early development of abrupt slope changes as the capsule content was increased. For instance, a change in the slope for the AM-0.125, AM-0.25, and AM-0.5 happened at 4500, 3500, and 2500 cycles, prior to the WTS range, to later stabilise at 9000, 8500 and 6000 cycles, respectively. As the number of cycles increases, no longer deformation is produced, due to a densification of the asphalt mixtures by the wheel passes. An earlier change in WTS indicates that the mixture was affected by the stripping phenomenon, i.e., the loss of adhesiveness between the aggregates and the asphalt binder. As example, Fig. 9b shows the final rutting state of the mixture samples at the end of the test (i.e., cycle 10,000). Regarding the impact of the alginate biopolymer on rutting resistance, Fig. 9a shows similar curves for the AM-0.250e and AM-0.0 samples, see Table 4.

**Table 4** Wheel tracking test parameters for each of the samples studied

| Sample | Initial height (mm) | RD (mm) | PRD (%) | WTS (mm/$10^{-3}$) |
|---|---|---|---|---|
| HMA-0.0 | 65.0 | 25.6 | 39.42 | 3.269 |
| HMA-0.125 | 64.7 | 31.2 | 48.21 | 3.807 |
| HMA-0.25 | 64.8 | 31.3 | 48.23 | 2.567 |
| HMA-0.5 | 64.7 | 32.8 | 50.69 | 0.490 |
| HMA-0.25e | 64.9 | 24.6 | 37.84 | 2.701 |

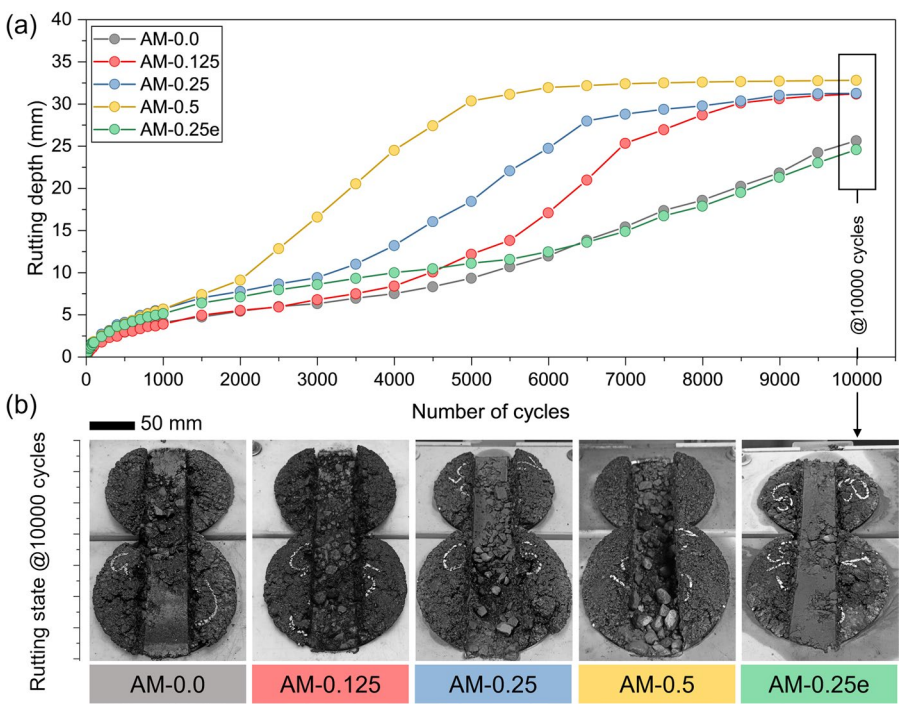


**Fig. 9** Results of wheel tracking tests: **a** Rutting depth (RD) curves for the AM samples with and without VCO capsules, and **b** final state of the asphalt mixtures at 10,000 cycles

This result aligns with the previously discussed adhesive property of alginate, which helps maintain the cohesion of mixture components over time. However, this effect diminishes with the gradual release of oil from the capsules, which softens the binder material and promotes reduced adhesion between aggregates and bitumen.

Based on the previous analysis, it can be concluded that the incorporation of VCO capsules into dense asphalt mixtures increased their susceptibility to rutting. This is evidenced by the occurrence of stripping at an earlier stage with increasing capsule content, attributed to higher VCO release. In summary, lower capsule dosages combined with enhanced stripping additives should be considered to manage rutting susceptibility when designing asphalt mixtures incorporating healing capsules. This previous evaluation of the physical and mechanical properties of the asphalt mixtures with, and without VCO capsules, suggests that there may be a partial release of encapsulated oil, which is proportional to the content of capsules in the mixture. This phenomenon resulted in softer bitumen, leading to asphalt mixtures that are more ductile and less resistant to mechanical stresses. Nonetheless, this effect is less pronounced in asphalt mixtures with 0.125%wt. of capsules (AM-0.125). Since the amount of oil released in the AM-0.125 samples is insufficient to markedly decrease their stiffness modulus and increase their ductility compared to a reference mixture (AM-0.0), it was concluded a capsule dosage of 0.125% wt. is optimal for evaluating the fatigue performance of the asphalt mixture. As a result, Fig. 10a and b displays the average results of fatigue tests of the initial and final at $N_{f50}$ condition for the stiffness modulus and phase angle results, respectively, for the AM-0.0 and AM-0.125 prismatic beams at 150, 190, and 300 microstrains.

Figure 10a shows that the stiffness modulus increased with the addition of VCO capsules and decreased with the increment of the microstrain level. At the same time, the phase angle decreased with the addition of VCO capsules and increased with the increment of the microstrain level, as shown in Fig. 10b. The increase in stiffness modulus and reduction in phase angle with the addition of VCO capsules in the asphalt mixture resulted in a more rigid bituminous material. This finding aligns with the analysis conducted from the ITS test and indicates that the encapsulated VCO, which may be partially released during manufacturing and compaction processes, does not negatively impact the fatigue life results. Conversely, the decrease in stiffness modulus and the increase in phase angle with the increase in microstrain levels indicate an increase in the viscous

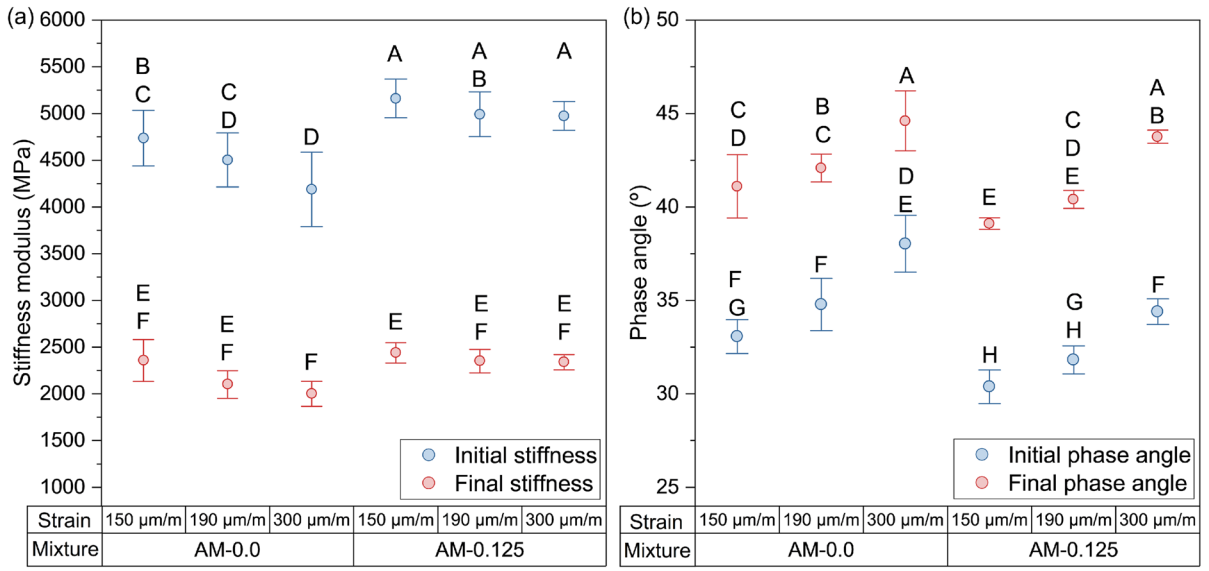


**Fig. 10** Average fatigue test results at Nf50 condition for the initial and final **a** stiffness modulus and **b** phase angle for the AM-0.0 and AM-0.125 prismatic asphalt beams. Mean values not sharing a capital letter (*A*, *B*, *C*, etc.) are statistically significant different ($p$-value < 0.05)

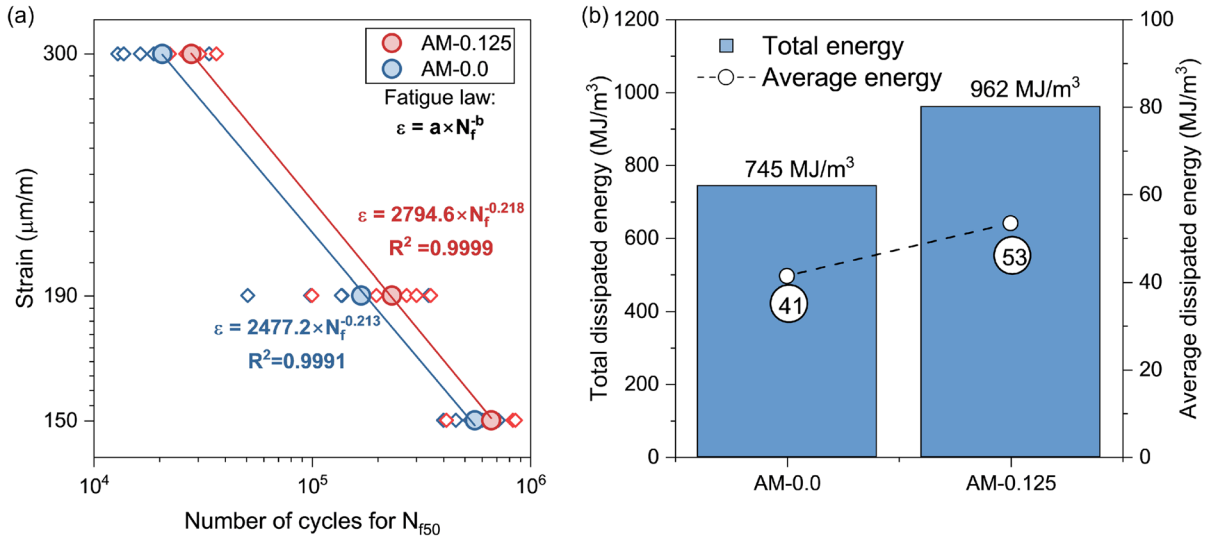


**Fig. 11** **a** Fatigue laws; and **b** Total and average dissipated energy for the AM-0.0 and AM-1.25 samples under a four-point bending test at 20 °C

**Table 5** Fatigue law parameters of the AM-0.0 and AM-0.125 evaluated per million cycles

| Asphalt mixture | a (μm/m) | b | ε ($10^6$) | $R^2$ |
|---|---|---|---|---|
| AM-0.0 | 2477.2 | − 0.213 | 130.61 | 0.9991 |
| AM-0.125 | 2794.6 | − 0.218 | 137.51 | 0.9999 |

component of the asphalt mixture. This leads to earlier deterioration of the test samples due to fatigue at the Nf50 condition.

Moreover, Fig. 11a presents the fatigue laws obtained for the AM-0.0 and AM-0.125 samples at 300, 190, and 150 microstrains. The results indicate that adding 0.125% wt. of VCO capsules had a beneficial effect on the fatigue resistance of the mixture, showing an average increase in the number of cycles of approximately 31% compared to the reference mixture without capsules. Furthermore, the fatigue resistance of the mixtures evaluated at one million cycles was characterised by the Fatigue Law, see Table 5. The strain values per million cycles (ε ($10^6$)) for the AM-0.0 and AM-0.125 mixtures were 130.61 and 137.51 μm/m, respectively, indicating that the mixtures with 0.125% wt. of VCO capsules increased their bending capacity and energy absorption when subjected to fatigue stress. Additionally, the respective fatigue laws of the asphalt mixtures showed a high correlation with the experimental data, as evidenced by the $R^2$ values of the linear fitting curves in Table 5.

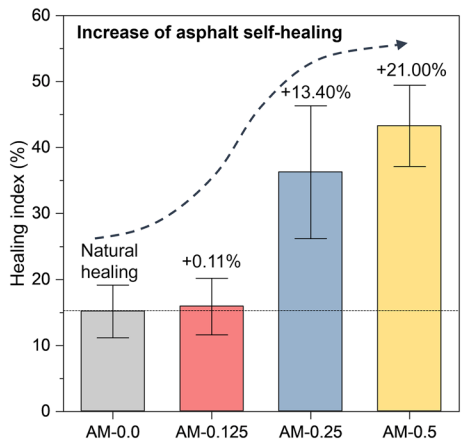


**Fig. 12** Average results of healing index and healing index improvement ratio parameter (see percentages) for asphalt mixtures with and without capsule addition

**Table 6** ANOVA *p*-values of the healing index for each asphalt mixture design

| Variable | *P*-value | Significant differences |
|---|---|---|
| *HI* | < 0.001 | AM-0.0–AM-0.25(0.5)<br>AM-0.125–AM-0.25(0.5)<br>AM-0.25–AM-0.5 |

Finally, the analysis of the fatigue test, presented in Fig. 11b, shows the accumulated and average

dissipated energy results. These results indicate that the AM-0.125 samples showed an increase of + 26% and + 29% in accumulated and average dissipated energy, respectively, compared to the AM-0.0 reference sample. This suggests that asphalt mixtures containing 0.125% wt. of VCO capsules require more mechanical work to induce fatigue failure in the samples. These results align with the observations made by Cheng et al. [58], who suggest that the fatigue life of an asphalt mixture is well correlated with the increase in accumulated dissipated energy. However, it is essential to note that studies on asphalt mixtures with capsules are relatively new and require further investigation.

### 3.3 Effect of the content of VCO capsules on the self-healing properties of asphalt mixtures

Optimised alginate capsules containing Virgin Cooking Oil (VCO) as an asphalt rejuvenator were prepared in this study for asphalt self-healing purposes. Figure 12a shows the average healing index (*HI*) measure for each asphalt mixture with values of 22.47% (SD: 6.17%), 22.58% (SD: 5.59%), 35.84% (SD: 10.06%), and 43.47% (SD: 6.17%) for the AM-0.0, AM-0.125, AM-0.25, and AM-0.5 test samples, respectively. Statistical results of ANOVA *p*-values indicate statistically significant differences between the asphalt mixtures with capsules and the reference one (without capsules), except for the AM-0.125 samples, as demonstrated in Table 6.

It should be noted that the previous healing indices for the asphalt mixtures containing capsules consider the intrinsic healing effect of the bitumen. With this in mind, to evaluate the contribution of the oil released from the capsules at each capsule dosage, a healing index improvement parameter was calculated as depicted in Eq. (9):

$$HR_n(\%) = HI_n - HI_0 \tag{9}$$

where $HR_n$ is the healing ratio of the asphalt test samples with a content of n% wt. of capsules, in %; $HI_n$ is the average healing index for samples with a content of n% wt. of capsules, in %; and $HI_0$ is the average healing index for the reference samples without capsules, in %.

Figure 12 shows the results of $HR_n$ with values of + 0.11%, + 13.40%, and + 21.00% for asphalt test samples with capsule contents of 0.125%wt., 0.25%wt., and 0.5% wt., respectively, indicating a significant increase in the healing level with a capsule content from 0.25%wt. or greater. These results can be explained by the capsule distribution inside the asphalt mixture previously analysed, see spatial capsule distribution in Fig. 5. At a low capsule content of 0.125%wt., the capsule dispersion inside the asphalt mixture leads to a lower capsule activation in the cracked zone, so the healing ability of the mixture behaves mainly as a reference mixture without capsules.

In contrast, when the capsule dosage is increased, they disperse throughout the asphalt mixture and form groups, leading to a higher number of capsules being activated in the cracked area. According to Norambuena-Conteras et al. [35], once the polynuclear capsules are activated within the asphalt mixture, the subsequent release and diffusion of the encapsulated rejuvenating agent led to a softening effect on the bitumen, allowing it to flow through the open crack and seal it. In conclusion, the previous analysis indicates that the self-healing capacity of the asphalt mixture is influenced by the distribution and quantity of capsules. In this study, the capsules were activated by the deformation mode resulting from the compressive load applied to the asphalt mixture samples. Therefore, dense asphalt mixtures with a higher capsule content are more likely to activate capsules in the cracked area, thereby enhancing their self-healing ability, as evidenced in Fig. 12.

## 4 Conclusions and future research

This study evaluated the effect of the content of an optimised biopolymer-based capsule design on the mechanical and self-healing properties of dense asphalt mixtures. A new approach was adopted to assess the spatial distribution of the capsules within the asphalt mixture and its impact on the mechanical and self-healing performance. From this work, the following conclusions were drawn:

- Capsules presented a better distribution as their % content was increased in the asphalt mixture, with a tendency to be grouped near the mixture's external zone. Overall, at a concentration

of 0.25% wt., the capsules exhibited a more uniform distribution.

- The addition of capsules led to a proportional increase in the bulk density of the asphalt mixtures, attributed to a decrease in the total air void content within the asphalt mixture.
- The addition of capsules resulted in decreased stiffness modulus values due to the release of oil, which softened the bitumen. The alginate matrix, however, functioned as a stiffening agent, contributing to an overall increase in the rigidity of the asphalt mixture.
- The addition of capsules exceeding 0.125% wt. reduced the low-temperature crack resistance, resulting in a more ductile behaviour post-failure due to the softening effect of the VCO released from the capsules. Additionally, the alginate matrix demonstrated adhesive properties.
- The susceptibility to water damage in the asphalt mixtures increased with the addition of capsules, suggesting a reduced adhesive capacity of the encapsulating biopolymer in water. However, this effect was mitigated by incorporating VCO into the biopolymeric alginate matrix.
- The presence of capsules in the asphalt mixtures led to earlier and deeper rutting due to the increased release of VCO, highlighting the necessity for additional research into adhesion promoter additives to address this issue.
- Asphalt mixtures with a capsule addition of 0.125% wt. exhibited improved resistance to fatigue damage and higher average stiffness modulus compared to a reference asphalt mixture. At higher strain values, mixtures containing VCO capsules showed increased ductility and energy absorption.
- Overall, asphalt samples with 0.125% wt. VCO capsules exhibited mechanical performance comparable to test samples without capsules; however, this content did not significantly enhance their self-healing properties. In contrast, self-healing capabilities were significantly enhanced with a capsule content greater than or equal to 0.25% wt.; however, this enhancement slightly affected some physical–mechanical properties of the dense asphalt mixture.

Based on the previous findings, future research could focus on evaluating: (1) The impact of adhesion promoters to enhance the mixture's performance against moisture damage. (2) The durability of asphalt mixtures with capsule additions in pavement structures using empirical mechanistic analysis. And (3) The influence of temperature variations and different healing rest periods on the self-healing properties of asphalt mixes incorporating optimised rejuvenating agents.

**Acknowledgements** The authors acknowledge Estefanía Paredes for her support during the experimental program and Jaime Zamorano from Gelymar S.A. for his assistance in the chemical characterisation of the alginate used in this study. The second author acknowledges financial support from the University of Bío-Bío through an internal PhD scholarship.

**Funding** This research was funded by the National Research and Development Agency (ANID) from Chile, through the Research Project FONDECYT Regular 2019 No.1190027.

**Data availability** The data that support the findings of this study are available from the corresponding author, [J.N–C], upon reasonable request.

**Declarations**

**Conflict of interest** The authors declare that they have no known competing financial interests or personal relationships that could have appeared to influence the work reported in this paper.



## References

1. Asphalt Institute, European Bitumen Association (2015) The bitumen industry: A global perspective, Third edition
2. Hunter R, Self A, Read J (2015) The Shell Bitumen Handbook, Sixth. Shell Bitumen, Westminster
3. Petersen JC (2009) A Review of the Fundamentals of Asphalt Oxidation Chemical, Physicochemical, Physical Property, and Durability Relationships. Washington D.C

4. Lesueur D (2009) The colloidal structure of bitumen: consequences on the rheology and on the mechanisms of bitumen modification. Adv Colloid Interface Sci 145:42–82. https://doi.org/10.1016/j.cis.2008.08.011
5. Morian N, Hajj EY, Glover CJ, Sebaaly PE (2011) Oxidative aging of asphalt binders in hot-mix asphalt mixtures. Transp Res Rec. https://doi.org/10.3141/2207-14
6. Airey GD (2003) State of the art report on ageing test methods for bituminous pavement materials. Int J Pavement Eng 4:165–176. https://doi.org/10.1080/10298430420000198568
7. Krolkral K, Haddadi S, Chailleux E (2020) Quantification of asphalt binder ageing from apparent molecular weight distributions using a new approximated analytical approach of the phase angle. Road Mater Pavement Des 21:1045–1060. https://doi.org/10.1080/14680629.2018.1536610
8. Miró R, Martínez AH, Moreno-Navarro F, del Carmen R-Gámez M (2015) Effect of ageing and temperature on the fatigue behaviour of bitumens. Mater Des 86:129–137. https://doi.org/10.1016/j.matdes.2015.07.076
9. Hofko B, Cannone Falchetto A, Grenfell J et al (2017) Effect of short-term ageing temperature on bitumen properties. Road Mater Pavement Des 18:108–117. https://doi.org/10.1080/14680629.2017.1304268
10. Kassem E, Khan MS, Katukuri S et al (2017) Retarding aging of asphalt binders using antioxidant additives and copolymers. Int J Pavement Eng 20:1154–1169. https://doi.org/10.1080/10298436.2017.1394098
11. Kanellopoulos A, Norambuena-Contreras J (2022) Self-healing construction materials. fundamentals, monitoring and large scale applications, First edition. Springer Nature Switzerland AG
12. Tabaković A, Schlangen E (2016) Self-healing technology for asphalt pavements. In: Hager M, van der Zwaag S, Schubert U (eds) Self-healing Materials. Springer international, Switzerland, pp 285–306
13. Sun D, Sun G, Zhu X et al (2018) A comprehensive review on self-healing of asphalt materials: mechanism, model, characterization and enhancement. Adv Colloid Interf Sci 256:65–93. https://doi.org/10.1016/j.cis.2018.05.003
14. Xu S, García A, Su J et al (2018) Self-healing asphalt review: from idea to practice. Adv Mater Interf. https://doi.org/10.1002/admi.201800536
15. Gonzalez-Torre I, Norambuena-Contreras J (2020) Recent advances on self-healing of bituminous materials by the action of encapsulated rejuvenators. Constr Build Mater 258:119568. https://doi.org/10.1016/j.conbuildmat.2020.119568
16. Alpizar-Reyes E, Concha JL, Martín-Martínez FJ, Norambuena-Contreras J (2022) Biobased spore microcapsules for asphalt self-healing. ACS Appl Mater Interf 14:31296–31311. https://doi.org/10.1021/acsami.2c07301
17. Norambuena-Contreras J, Concha JL, Arteaga-Pérez LE, Gonzalez-Torre I (2022) Synthesis and characterisation of alginate-based capsules containing waste cooking oil for asphalt self-healing. Appl Sci 12:2739. https://doi.org/10.3390/app12052739
18. Norambuena-Contreras J, Arteaga-Pérez LE, Concha JL, Gonzalez-Torre I (2021) Pyrolytic oil from waste tyres as a promising encapsulated rejuvenator for the extrinsic self-healing of bituminous materials. Road Mater Pavement Des 22:S117–S133. https://doi.org/10.1080/14680629.2021.1907216
19. Behnood A (2019) Application of rejuvenators to improve the rheological and mechanical properties of asphalt binders and mixtures: a review. J Clean Prod 231:171–182. https://doi.org/10.1016/j.jclepro.2019.05.209
20. Xu S, Liu X, Tabaković A, Schlangen E (2020) A novel self-healing system: towards a sustainable porous asphalt. J Clean Prod 259:120815. https://doi.org/10.1016/j.jclepro.2020.120815
21. Li Y, Hao P, Zhang M (2021) Fabrication, characterization and assessment of the capsules containing rejuvenator for improving the self-healing performance of asphalt materials: a review. J Clean Prod 287:125079. https://doi.org/10.1016/j.jclepro.2020.125079
22. Al-Mansoori T, Norambuena-Contreras J, Garcia A (2018) Effect of capsule addition and healing temperature on the self-healing potential of asphalt mixtures. Mater Struct/Materiaux et Constructions. https://doi.org/10.1617/s11527-018-1172-5
23. Bao S, Liu Q, Li H et al (2021) Investigation of the release and self-healing properties of calcium alginate capsules in asphalt concrete under cyclic compression loading. J Mater Civil Eng. https://doi.org/10.1061/(asce)mt.1943-5533.0003517
24. Norambuena-Contreras J, Yalcin E, Hudson-Griffiths R, García A (2019) Mechanical and self-healing properties of stone mastic asphalt containing encapsulated rejuvenators. J Mater Civil Eng. https://doi.org/10.1061/(asce)mt.1943-5533.0002687
25. Rao W, Liu Q, Yu X et al (2021) Efficient preparation and characterization of calcium alginate-attapulgite composite capsules for asphalt self-healing. Constr Build Mater. https://doi.org/10.1016/j.conbuildmat.2021.123931
26. Ruiz-Riancho N, Traseira Piñeiro L, Abedraba Abdalla M, Garcia A (2022) Encapsulated bitumen rejuvenators for reflective cracking and ravelling mitigation. In: Eleventh International conference on the bearing capacity of roads, railways and airfields, Volume 2. CRC Press, pp 201–209
27. Wan P, Wu S, Liu Q et al (2022) Sustained-release calcium alginate/diatomite capsules for sustainable self-healing asphalt concrete. J Clean Prod. https://doi.org/10.1016/j.jclepro.2022.133639
28. Wang H, Liu Q, Wu J et al (2023) Self-healing performance of asphalt concrete with Ca-alginate capsules under low service temperature conditions. Polymers. https://doi.org/10.3390/polym15010199
29. Xu S, Tabaković A, Liu X et al (2019) Optimization of the calcium alginate capsules for self-healing asphalt. Appl Sci. https://doi.org/10.3390/app9030468
30. Concha JL, Arteaga-Pérez LE, Gonzalez-Torre I et al (2022) Biopolymeric capsules containing different oils as rejuvenating agents for asphalt self-healing: a novel multivariate approach. Polymers. https://doi.org/10.3390/polym14245418
31. Wan P, Wu S, Liu Q et al (2022) Recent advances in calcium alginate hydrogels encapsulating rejuvenator for asphalt self-healing. J Road Eng 2:181–220. https://doi.org/10.1016/j.jreng.2022.06.002

32. De Bock L, Piérard N, Vansteenkiste S, Vanelstraete A (2020) Dossier 21. Categorisation and analysis of rejuvenators for asphalt recycling. Belgian Road Research Centre, Brusels
33. Concha JL, Arteaga-Pérez LE, Alpizar-Reyes E et al (2022) Effect of rejuvenating oil type on the synthesis and properties of alginate-based polynuclear capsules for asphalt self-healing. Road Mater Pavement Des. https://doi.org/10.1080/14680629.2022.2092026
34. Al-Mansoori T, Micaelo R, Artamendi I et al (2017) Microcapsules for self-healing of asphalt mixture without compromising mechanical performance. Constr Build Mater 155:1091–1100. https://doi.org/10.1016/j.conbuildmat.2017.08.137
35. Norambuena-Contreras J, Yalcin E, Garcia A et al (2018) Effect of mixing and ageing on the mechanical and self-healing properties of asphalt mixtures containing polymeric capsules. Constr Build Mater 175:254–266. https://doi.org/10.1016/j.conbuildmat.2018.04.153
36. Zhang L, Liu Q, Li H et al (2019) Synthesis and characterization of multi-cavity Ca-alginate capsules used for self-healing in asphalt mixtures. Constr Build Mater 211:298–307. https://doi.org/10.1016/j.conbuildmat.2019.03.224
37. Ruiz-Riancho N, Saadoon T, Garcia A et al (2021) Optimisation of self-healing properties for asphalts containing encapsulated oil to mitigate reflective cracking and maximize skid and rutting resistance. Constr Build Mater. https://doi.org/10.1016/j.conbuildmat.2021.123879
38. Garcia-Hernández A, Salih S, Ruiz-Riancho I et al (2020) Self-healing of reflective cracks in asphalt mixtures by the action of encapsulated agents. Constr Build Mater. https://doi.org/10.1016/j.conbuildmat.2020.118929
39. Traseira-Piñeiro L, Parry T, Haughey F, Garcia-Hernandez A (2022) Performance of plant-produced asphalt containing cellular capsules. Materials. https://doi.org/10.3390/ma15238404
40. Concha JL (2023) Optimised Alginate-Based Capsules Containing Vegetal Oils as Rejuvenators for Asphalt Self-Healing. PhD Thesis, Universidad del Bío-Bío
41. Ministerio de Obras Públicas (2022) Manual de carreteras. Volumen nº 5. Especificaciones técnicas generales de construcción
42. Concha JL, Viana-Sepulveda A, Caro S et al (2024) Dynamic mechanical analysis of asphalt mortar samples containing millimetre-size capsules for self-healing purposes. Powder Technol 440:119735. https://doi.org/10.1016/j.powtec.2024.119735
43. Concha JL, Delgadillo R, Arteaga-Pérez LE et al (2023) Optimised sunflower oil content for encapsulation by vibrating technology as a rejuvenating solution for asphalt self-healing. Polymers 15:1578. https://doi.org/10.3390/polym15061578
44. BS-EN 12697-30:2018 (2018) Part 30: Specimen preparation by impact compactor
45. BS-EN 12697-33:2003 (2003) Part 33: Specimen prepared by roller compactor
46. BS-EN 12697-24:2012 (2012) Part 24: Resistance to fatigue
47. ASTM D-2726-00 (2000) Standard Test Method for Bulk Specific Gravity and Density of Non-Absorptive Compacted Bituminous Mixtures. West Conshohocken, PA, USA
48. ASTM D3203-05 (2005) Standard Test Method for Percent Air Voids in Compacted Dense and Open Bituminous Paving Mixtures. West Conshohocken, PA, USA
49. BS-EN 12697-26:2004 (2004) Part 26: Stiffness
50. Valdés-Vidal G, Calabi-Floody A, Miró-Recasens R, Norambuena-Contreras J (2015) Mechanical behavior of asphalt mixtures with different aggregate type. Constr Build Mater 101:474–481. https://doi.org/10.1016/j.conbuildmat.2015.10.050
51. BS-EN 12697-23:2017 (2017) Part 23: Determination of the Indirect tensile strength of bituminous specimens
52. BS-EN 12697-12:2003 (2004) Part 12: Determination of the water sensitivity of bituminous specimens
53. AASHTO T 324-14 (2014) Standard Method of Test for Hamburg Wheel-Track Testing of Compacted Hot Mix Asphalt (HMA)
54. Concha JL, Sáez-Gutierrez M, Norambuena-Contreras J (2024) Mechanical activation assisted of biobased encapsulated rejuvenators to promote asphalt self-healing. Mater Today Commun 38:107735. https://doi.org/10.1016/j.mtcomm.2023.107735
55. Nafidi A, Bahij M, Achchab B, Gutiérrez-Sanchez R (2019) The stochastic Weibull diffusion process: computational aspects and simulation. Appl Math Comput 348:575–587. https://doi.org/10.1016/j.amc.2018.12.017
56. Lupo B, Maestro A, Gutiérrez JM, González C (2015) Characterization of alginate beads with encapsulated cocoa extract toprepare functional food: comparison of two gelation mechanisms. Food Hydrocoll 49:25–34. https://doi.org/10.1016/j.foodhyd.2015.02.023
57. Hasnain MS, Jameel E, Mohanta B, et al (2020) Alginates in Drug Delivery. Andre Gerhard Wolff, Chennai
58. Cheng H, Sun L, Wang Y et al (2022) Fatigue test setups and analysis methods for asphalt mixture: a state-of-the-art review. J Road Eng 2:279–308. https://doi.org/10.1016/j.jreng.2022.11.002